Effect of AlN buffer layer properties on the morphology and polarity of GaN nanowires grown by molecular beam epitaxy

Matt D. Brubaker,[1,2,3,a)] Igor Levin,[4] Albert V. Davydov,[4] Devin M. Rourke,[1] Norman A. Sanford,[1] Victor M. Bright,[2,3] and Kris A. Bertness[1]
[1]*Physical Measurement Laboratory, National Institute of Standards and Technology, Boulder, Colorado 80305, USA*
[2]*Department of Mechanical Engineering, University of Colorado, Boulder, Colorado 80309, USA*
[3]*DARPA Center for Integrated Micro/Nano-Electromechanical Transducers (iMINT), University of Colorado, Boulder, Colorado 80309, USA*
[4]*Material Measurement Laboratory, National Institute of Standards and Technology, Gaithersburg, Maryland 20899, USA*

(Received 17 June 2011; accepted 3 August 2011; published online 8 September 2011)

Low-temperature AlN buffer layers grown via plasma-assisted molecular beam epitaxy on Si (111) were found to significantly affect the subsequent growth morphology of GaN nanowires. The AlN buffer layers exhibited nanowire-like columnar protrusions, with their size, shape, and tilt determined by the AlN V/III flux ratio. GaN nanowires were frequently observed to adopt the structural characteristics of the underlying AlN columns, including the size and the degree of tilt. Piezoresponse force microscopy and polarity-sensitive etching indicate that the AlN films and the protruding columns have a mixed crystallographic polarity. Convergent beam electron diffraction indicates that GaN nanowires are Ga-polar, suggesting that Al-polar columns are nanowire nucleation sites for Ga-polar nanowires. GaN nanowires of low density could be grown on AlN buffers that were predominantly N-polar with isolated Al-polar columns, indicating a high growth rate for Ga-polar nanowires and suppressed growth of N-polar nanowires under typical growth conditions. AlN buffer layers grown under slightly N-rich conditions (V/III flux ratio = 1.0 to 1.3) were found to provide a favorable growth surface for low-density, coalescence-free nanowires. © *2011 American Institute of Physics*. [doi:10.1063/1.3633522]

I. INTRODUCTION

AlN buffer layers are commonly employed in the growth of high quality GaN films on non-native substrates. Whereas it is generally observed that a smooth AlN buffer layer grown via MBE near stoichiometric flux conditions is beneficial for GaN epilayers,[1,2] it is less clear whether a smooth AlN buffer layer is preferred for GaN nanowire growth. Low-temperature AlN buffer layers grown on silicon frequently exhibit a rough columnar microstructure[3] with nanowire-like features that might act as nucleation sites for subsequent GaN nanowires. In fact, several groups have reported a strong dependence of GaN nanowire morphology on the characteristics of the AlN buffer layer,[4–7] which at least potentially enables some level of control over the shape, diameter, and density of nanowires. The sensitivity of the nanowire morphology to the AlN growth surface underscores the role of the nanowire nucleation process and implies that a "seeded" nucleation process might be active in addition to the "spontaneous" shape change/plastic deformation nucleation process described by others.[5,8]

AlN buffer layers are also utilized to impart a preferred crystallographic polarity onto subsequent GaN layers, most notably for GaN/sapphire.[9] However, for the heteroepitaxial growth of III-nitrides on non-polar Si(111), there is no *a priori* expectation for a preferred AlN polarity, which was reported to depend on growth conditions including the V/III ratio,[10,11] growth temperature and surface reconstructions,[12] and initial dose of Al or N.[3,13] Thus, it is important to experimentally establish the AlN polarity and reveal its effects on GaN nanowire morphology. Indeed, mixed-polarity GaN nanowires growing from a film-like N-polar "matrix" or "compact" GaN layer have been reported elsewhere and were speculated to result from the underlying AlN polarity.[14] A polarity-dependent growth rate was also observed[15] and was attributed to a high-temperature growth limitation for N-polar GaN,[16] suggesting a potential mechanism for suppressing the growth of N-polar material. This variation in growth kinetics could in theory be used to preferentially grow Ga-polar GaN nanowires, which are expected to exhibit a more favorable Mg incorporation efficiency similar to that of Ga-polar Mg:GaN epilayers.[17]

High defect densities associated with low-temperature AlN growth can complicate the measurement of film polarity, particularly for diffraction-based techniques such as convergent beam electron diffraction (CBED). Polarity-sensitive etching is also dependent on defect densities; thus we employed piezoresponse force microscopy (PFM) measurements to provide supplemental information about the AlN buffer layer polarity and surface topography. PFM allows for direct measurement of the actual growth surface, in contrast to polarity-sensitive etching, which might lift off features of interest. PFM is an AFM-based imaging technique in which

a)Author to whom correspondence should be addressed. Electronic mail: matthew.brubaker@nist.gov.

the tip is electrically biased with an ac signal in order to induce piezoelectric deformation in the sample, which is then detected through the cantilever deflection via a lock-in amplifier. The phase of the deflection signal with respect to the bias signal determines the polarity in nitride materials,[18–20] with metal-polarity exhibiting in-phase behavior and N-polarity exhibiting out-of-phase behavior.

In this work, we investigate the role of the low-temperature AlN buffer layer in GaN nanowire nucleation. The aim of this study was to identify buffer layer characteristics that facilitate the growth of low density, straight, coalescence-free nanowires. AlN buffer layers were grown under varying V/III flux ratios in order to produce a range of structural and polarity configurations, which were characterized using complementary techniques. A companion set of GaN nanowire samples grown on similar buffer layers provided correlation between the AlN characteristics and the GaN nanowire morphology.

II. EXPERIMENTS

AlN buffer layers and GaN nanowire samples were grown on n-type low-resistivity silicon (111) substrates by use of a home-built, plasma-assisted MBE system. Conventional effusion sources were used for group III elements, and a commercial rf plasma source was used to supply active nitrogen. Group III fluxes were characterized via ionization gauge measurements calibrated against the Al/Ga-limited linear regime of the growth-rate curves. The film growth rates were measured via *in situ* reflectance measurements and/or *ex situ* field-emission scanning electron microscopy (FESEM) imaging and were estimated to be within $\pm 15\%$, depending on the variation of the surface topography. AlN V/III flux ratios were estimated to be $\pm 20\%$ and were calculated using an active nitrogen flux determined from the transition between N-rich and Al-rich conditions. Substrate temperatures were measured via pyrometry at the backside of the wafer surface and were calibrated against frontside pyrometer measurements of a bare silicon wafer. The uncertainty of this approach was previously estimated to be $8\,^{\circ}\mathrm{C}$.[21]

The silicon substrates were cleaned with a dilute HF solution (1:10 HF:H_2O) and then outgassed for 1 h in a load-lock chamber equipped with a quartz lamp for radiant heating. After introduction into the growth chamber, the wafer was outgassed for an additional 15 min at $910\,^{\circ}\mathrm{C}$ to remove any residual oxide. AlN buffer layers were then grown using various V/III flux ratios at a substrate temperature of $630\,^{\circ}\mathrm{C}$. An initial 13 s dose of Al was deposited at $680\,^{\circ}\mathrm{C}$ prior to striking the rf plasma in order to suppress nitridation of the silicon surface. This initial dose corresponded to approximately 1 to 3 monolayers for the range of Al fluxes used in these experiments. A plasma power of 350 W and a nitrogen flow rate of 1.0 SCCM (SCCM denotes cubic centimeters per minute at standard temperature and pressure) were used for all AlN buffer layers. Mg-doped GaN nanowires were grown under nominally N-rich conditions with a Ga flux of 2.6 to $3.1 \times 10^{13}\ \mathrm{cm^{-2}\ s^{-1}}$; a Mg cell temperature of $370\,^{\circ}\mathrm{C}$; and 400 W, 1.0 SCCM nitrogen plasma conditions. A two-stage temperature schedule was used for the nanowire growth, comprising 2 h at $820\,^{\circ}\mathrm{C}$ followed by 12 h at $800\,^{\circ}\mathrm{C}$.

The morphologies of the AlN buffer layers and the nanowire samples were observed by use of FESEM and TEM. The crystallographic polarity of the AlN films and the GaN nanowire samples was characterized via a suite of measurements including polarity-sensitive etching, PFM, and CBED. Hot phosphoric acid at various temperatures ($75\,^{\circ}\mathrm{C}$ to $125\,^{\circ}\mathrm{C}$) was utilized for polarity-sensitive etch tests on the AlN films and GaN nanowire samples. AlN N-polar regions revealed pyramidal etch figures with a hexagonal basal plane. The orientation and sidewall angles of the pyramidal structures indicate that the pyramids are bounded by {10-11} planes, consistent with literature reports for etched N-polar AlN.[22] Al-polar AlN produced a surface with hexagonal pits and etched at an overall slower rate than N-polar material. In mixed polarity AlN films, the slow-etching Al-polar domains were often observed as protrusions from the N-polar pyramidal structures, similar to what is described in previous reports.[23] CBED measurements were performed on a GaN nanowire cross-sectional TEM sample prepared via mechanical polishing and ion milling. CBED was accomplished in a Phillips CM-30 TEM operated at 100 kV and with a sample temperature of 100 K. The CBED simulations were performed using Bloch wave calculations implemented in the JavaScript version of the EMS code.

PFM measurements were carried out by use of a commercial AFM system and an external lock-in amplifier coupled to the AFM deflection signal. A conductive diamond AFM tip was used as the top electrode and the silicon wafer served as the bottom electrode for the PFM setup. The tips had a force constant of 5 N/m and were biased at 5 V_{rms} and a frequency of 10 kHz, far from the cantilever resonant frequency of 118 kHz. Several measurement artifacts have been reported to introduce 180° phase offsets, complicating the direct interpretation of phase data, including electrostatic interactions,[24,25] cantilever buckling effects,[26] and the laser position on the cantilever.[27] Whether these artifacts are operative or not depends largely on the specific measurement conditions, including the cantilever spring constant and the tip-sample capacitance gradient, which in turn depend on the film thickness and surface depletion layers. In order to eliminate these bias-dependent ambiguities, we benchmarked PFM phase measurements against polarity-sensitive etch tests by use of films with predominant Al-polarity or N-polarity. It was found that the PFM phase could be modulated between 0° and 180° depending on the dc bias (V_{dc}) applied to the tip, indicating a non-negligible electrostatic contribution to the piezoresponse signal. Empirically, it was found that PFM yields the correct polarity at $V_{dc} = 0$ V, provided that a 180° phase offset is applied.

A similar experiment was performed on a film of mixed polarity by correlating as-grown, PFM, and post-etch images for the same location on the sample (Fig. 1). The tip radius was found to be significant in proportion to the domain size, and thus the spatial resolution in the topography and phase images was limited by the tip-imaging artifact. For domains larger than the tip radius, PFM yields the correct polarity by

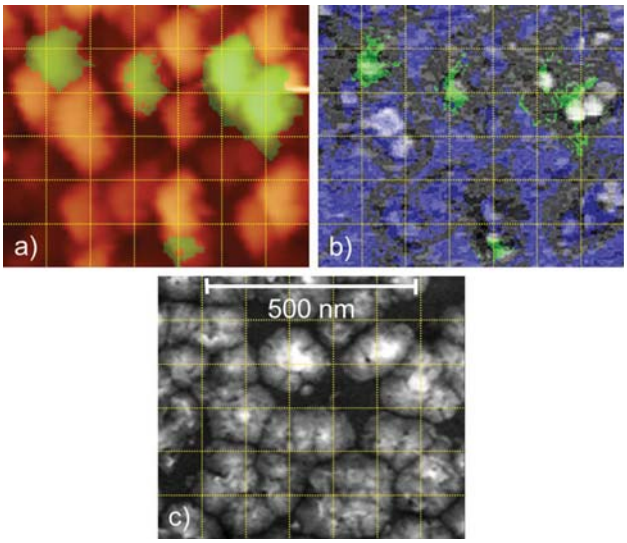

FIG. 1. (Color) Correlation of the PFM measurement of an as-grown surface (a), a FESEM image of an as-grown surface (b), and a FESEM image of a post-polarity-sensitive etch surface (c) for the same location on an AlN buffer layer. The PFM image shows the topography (brown) with a phase overlay (green = Al-polar, unmarked = N-polar). The as-grown FESEM image has a PFM phase overlay with the tip image artifacts removed (green = Al-polar, blue = N-polar, unmarked = data removed due to tip imaging).

use of the $V_{dc} = 0$ V, 180° phase offset convention; however, erroneous PFM phase information was observed in regions where tip imaging dominates, such as pinholes or areas proximal to protruding columns. Tip shape analysis and certainty mapping algorithms were used in this cross-correlation experiment in order to improve the data quality via the identification of regions subject to tip imaging and the removal of associated data from the PFM phase image [Fig. 1(b)]. Interestingly, some Al-polar regions identified via PFM did not survive the polarity-sensitive etch, but they left a visible crater behind, indicating that the domain might have been undercut and lifted off during etching. It was also observed that protruding columns exhibit both polarity types, which precludes the possibility that the phase contrast is solely due to a topographic artifact.

III. RESULTS AND DISCUSSION

A. AlN buffer layer

A series of thicker AlN samples was grown at various Al cell temperatures for the analytical characterization of the film morphology, crystallographic structure, and polarity. The growth duration for each particular V/III flux ratio was adjusted so that the final film thickness was approximately 100 nm, allowing for greater development of the microstructure than does the typical 40 nm thickness used for nanowire growth. The AlN growth rate varied as a function of the Al flux and exhibited the expected linear N-rich regime and the plateau-like Al-rich regime.[1] An abrupt transition was observed between N-rich and Al-rich conditions, which likely reflects the relatively low substrate temperature and negligible re-evaporation of Al.[2] The transition between these regimes delineates the stoichiometric flux condition (V/III ratio = 1) and indicates an active nitrogen flux of approximately 1.6 to 1.7×10^{14} cm^{-2} s^{-1}, which supported a maximum AlN growth rate of approximately 2 nm/min. XRD measurements of films grown under slightly N-rich conditions (not shown) indicate a wurtzite structure with the expected epitaxial relationship $(0001)_{AlN} \| \{111\}_{Si}$, $<10\text{-}10>_{AlN} \| <11\text{-}2>_{Si}$.

The morphology and polarity of the AlN buffer layers can be categorized as very N-rich, slightly N-rich, and Al-rich conditions. Columnar features were observed to protrude from a finer grained film layer [Figs. 2(a)–2(c)]. The columns exhibit a nanowire-like structure with approximately *m*-plane sidewalls and a hexagonal top face of varying irregularity. This nanowire-like structure suggests that subsequent GaN nanowires might propagate from existing AlN columns. For very N-rich conditions (V/III ratio = 1.7) the columns are misoriented relative to the substrate normal by up to 15° and are substantially taller than the surrounding film. Others have also observed similar results under very N-rich conditions, manifest in high values of FWHM in XRD rocking-curve measurements.[1,28] With increasing Al flux into slightly N-rich conditions ($1.3 \geq$ V/III ratio > 1), the columns align with the substrate normal and decrease in height relative to the film surface, ultimately becoming smooth near

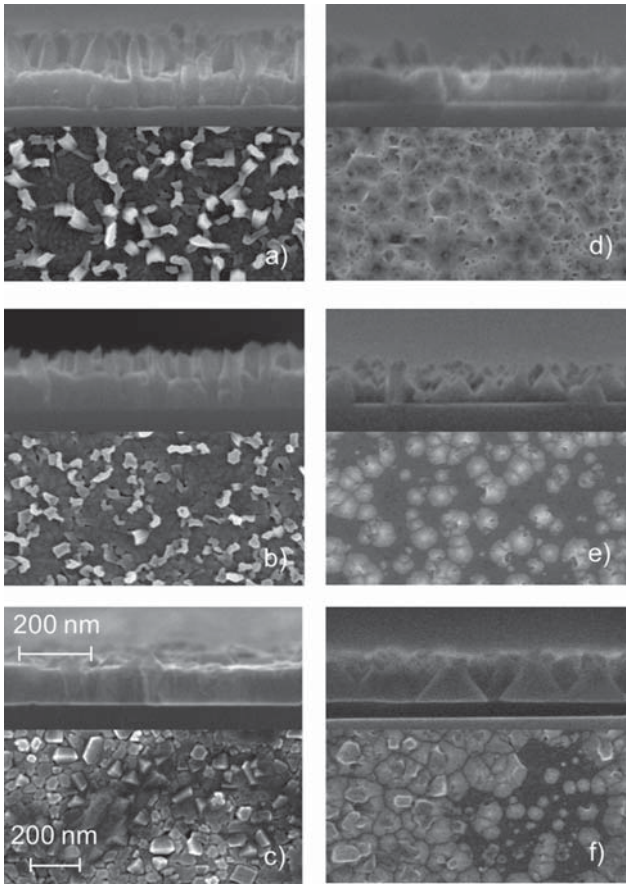

FIG. 2. Plan and cross-sectional FESEM images of as-grown [(a)-(c)] and polarity-sensitive etched [(d)-(f)] AlN films grown under [(a) and (d)] very N-rich conditions (V/III flux ratio = 1.7), [(b) and (e)] slightly N-rich conditions (V/III flux ratio = 1.3), and [(c) and (f)] Al-rich conditions (V/III flux ratio = 0.8).

the stoichiometric flux condition. Under Al-rich conditions (V/III ratio < 1), Al droplets are observed, the overall grain size increases, and larger platelet structures emerge. A fraction of the taller grains in the Al-rich region are observed to elongate along the <11-20> directions and have inclined facets on the top surface.

Polarity-sensitive etching [Figs. 2(d)–2(f)] and PFM measurements [Figs. 3(a)–3(c)] produced similar results, as summarized in Table I. The protruding columns exhibit mixed polarity in all samples, with only a small fraction of Al-polar columns under very N-rich conditions and a substantially higher fraction under Al-rich conditions. The mean diameter of the Al-polar columns also increases with the Al flux, from 30 to 40 nm under N-rich conditions to 70 to 85 nm under Al-rich conditions. The tendency for Al-rich conditions to produce Al-polarity films has been observed by others[10] and was speculated to result from Al–Al bonding and a subsequent flip in the polarity. Under most conditions, the surrounding film is observed to have N-polarity, with the exception of Al-polarity being observed under very N-rich conditions. It is not presently clear why decreasing the Al flux causes the surrounding film layer to change from N-polarity to Al-polarity. It is possible that the higher Al-prelayer dose for increased Al fluxes plays a role in seeding the N-polar configuration, as reported elsewhere.[13] This behavior of AlN polarity contrasts with results from another MBE system in our lab that yields smooth, predominantly Al-polar AlN under similar growth conditions.[21]

B. GaN nanowires

A separate series of GaN nanowire samples was grown in order to investigate the effect of the AlN buffer V/III ratio on the nanowire morphology. The AlN thickness was fixed at 40 nm by reducing the total growth time, and the Al flux was varied in order to yield very N-rich to Al-rich conditions. AlN buffers grown under very N-rich conditions (V/III ratio = 1.7) yield thin nanowires [Figs. 4(a) and 4(d)] with a diameter comparable to that of the Al-polar columns remaining after polarity-sensitive etching (~30 nm). The nanowire density (1 to 2 μm^{-2}) is significantly less than the total AlN column density (50 μm^{-2}), indicating that nanowire growth does not occur solely as a result of the continuation of growth at the AlN column tips. Also observable is a high density of short nanowire nuclei, usually located at the center of a hexagonal pit [Figs. 4(a) and 4(d)]. These nuclei do not grow thicker than a few tens of nanometers at typical nanowire growth temperatures, regardless of the growth duration, similar to the surrounding matrix layer. The density of the shorter nanowire nuclei is much higher (50 μm^{-2}) and is roughly equivalent to the AlN column density. These results suggest that the AlN columns act as nucleation sites for nanowire growth, as mentioned earlier, but will grow to appreciable length only on the small fraction of Al polar columns. Considering that nanowire growth occurs at only 20 °C below the temperature of "no growth conditions," it is possible that a high-temperature limitation for N-polar GaN (Ref. 16) is suppressing growth on the N-polar fraction of the AlN columns, similar to the dependence of the nanowire growth rate on the polarity that has been reported elsewhere.[15] Lastly, many nanowires can be observed to be tilted (up to 20°) with respect to the substrate normal, similar to the misorientation observed for columns in AlN layers grown under similar conditions. This tilting often leads to an unacceptable level of coalescence for longer nanowire growths.

Increasing the Al flux to slightly N-rich conditions (V/III ratio = 1.3) causes the nanowires to align with the substrate normal [Figs. 4(b) and 4(e)], similar to what occurs with AlN columns under similar conditions as described above. TEM images corroborate this observation and further illustrate that there is no tapering of the nanowire sidewalls [Fig. 5(a)]. Nanowires fabricated under these conditions were grown coalescence-free up to 9 μm and were limited only by the growth time. In many cases, the cross-sectional shape of the nanowires deviates from the ideal hexagonal structure and is preserved along the full length of the nanowire. This result implies that the asymmetric cross-sectional shape of the nanowires is determined at the nucleation stage, likely from the irregular shape of the AlN columns in the buffer layer. The length is observed to vary among nanowires and does not follow the inverse radius relationship observed by others[29] or the near homogenous lengths observed with a different growth system in our lab.[21] Although shadowing effects could account for random variation in the growth length, it seems unlikely that this is the case for such low nanowire densities. It is not presently clear whether this dispersion in length is due to delayed nucleation or differential growth rates between nanowires. It is also unclear why many but not all nanowires have a facetted tip surface [Fig. 5(a)]. Similar to nanowire growths on very N-rich AlN buffers, there is a high density of short (less than 50 nm) nanowire nuclei growing in hexagonal pits in addition

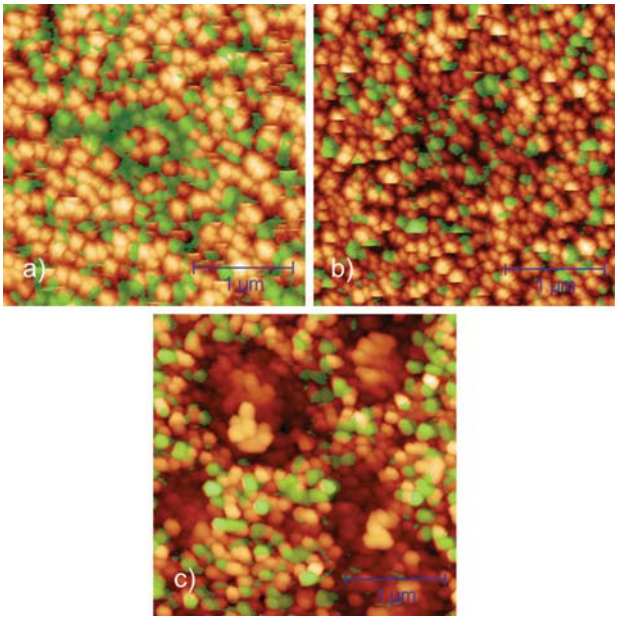

FIG. 3. (Color) PFM images of the AlN film topography (brown) and the PFM phase overlay (green = Al-polar, unmarked = N-polar) corresponding to (a) very N-rich conditions (V/III flux ratio = 1.7), (b) slightly N-rich conditions (V/III flux ratio = 1.3), and (c) Al-rich conditions (V/III flux ratio = 0.8). The *z*-height scale is 150 nm for (a), 105 nm for (b), and 45 nm for (c).

TABLE I. Summary of polarity measurements for AlN buffer layers and GaN nanowire samples.

Layer	Growth conditions	V/III flux ratio	Polarity sensitive etching	PFM	CBED
AlN	Very N-rich	1.7	Film: Al-polar; columns: ~30% Al-polar	Film: Al-polar; columns: ~20% Al-polar	–
	Slightly N-rich	1.0–1.3	Film: N-polar; columns: ~20% Al-polar	Film: N-polar; columns: ~20% Al-polar	–
	Al-rich	0.8–1.0	Film: N-polar; columns: ~70% Al-polar	Film: N-polar; columns: ~50% Al-polar	–
GaN matrix	Slightly N-rich	1.3	N-polar	–	–
GaN nanowires		1.3	–	–	Ga-polar

to the low density longer nanowires. It should be noted that the associated buffer layer shows a similarly proportionate density of N-polar and Al-polar columns, supporting the hypothesis that the bimodal nanowire morphology results from the AlN buffer polarity.

GaN nanowires on AlN buffers grown near the stoichiometric flux condition show a marked change in morphology, with a substantial increase in the overall nanowire size and surface fill factor [Figs. 4(c) and 4(f)]. The nanowire cross sections are very irregular, yet they still retain the sidewall faceting and axial homogeneity observed in N-rich AlN samples, illustrating the templating effect of the underlying AlN buffer layer. Unlike in N-rich AlN samples, the nanowire diameter exceeds the Al-polar column diameter, possibly as a result of excess Al that accumulates on the surface under Al-rich conditions. This excess Al might convert to AlN during the ramp to nanowire growth temperatures, creating a thin layer of AlN overgrowth. During this growth interruption, the N shutter remains open, exposing the growth surface to an equivalent N flux approximately five times higher than the excess Al flux. It is uncertain whether this AlN overgrowth was resolved in the AlN polarity measurements described above. The abrupt transition between N-rich and Al-rich conditions at low AlN growth temperatures causes the morphology to be hypersensitive at the stoichiometric flux condition. This instability is further compounded by variations in the active nitrogen flux resulting from plasma start-up transients and the long term clogging of plasma exit apertures.

CBED analysis was carried out on the nanowire sample grown on slightly N-rich AlN (V/III flux ratio = 1.3). The CBED pattern and simulation [Figs. 5(b) and 5(c)] for a long nanowire indicate Ga-polarity, supporting the hypothesis that the longer nanowires are Ga-polar. The AlN layer was too defective to allow us to obtain a well-defined diffraction pattern, prohibiting the direct correlation of AlN and GaN polarity for a given nanowire. Likewise, the quality of the CBED patterns recorded from the short nanowire nuclei was insufficient for an unambiguous determination of the polarity. Polarity-sensitive etching of GaN nanowires produced similarly inconclusive results, with tapering observed at both the root and the tip of the nanowire. It is likely that the tip faceting in as-grown nanowires precludes a reliable examination of the etch effects, a shortcoming that is compounded by the limited resolution of FESEM imaging.

In order to resolve the matrix layer polarity, a low-temperature nanowire growth (730 °C to 780 °C) on slightly N-rich AlN was carried out to encourage thick matrix layer growth for polarity-sensitive etching. Although these conditions were more typical for planar film growth, there was

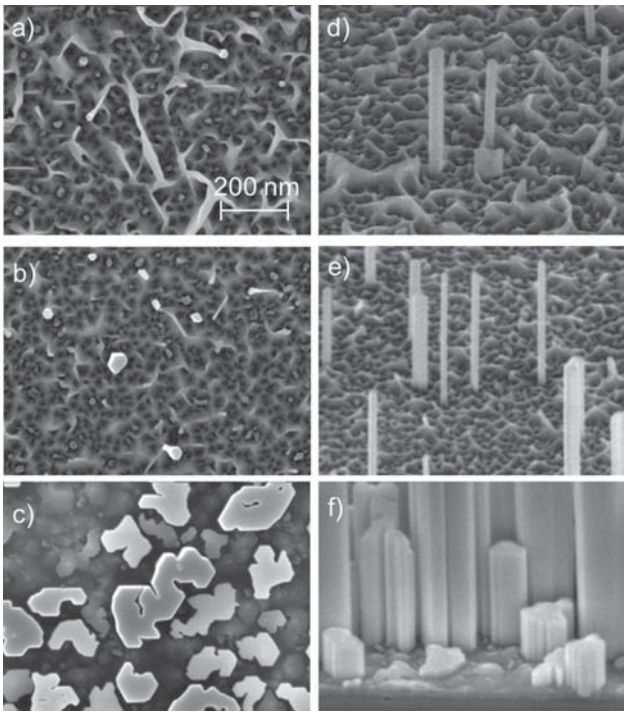

FIG. 4. FESEM images in plan view [(a)-(c)] and 40° tilt view [(d)-(f)] showing the morphology of GaN nanowires grown on AlN buffer layers with Al/N flux ratios corresponding to [(a) and (d)] very N-rich conditions (V/III flux ratio = 1.7), [(b) and (e)] slightly N-rich conditions (V/III flux ratio = 1.3), and [(c) and (f)] near stoichiometric flux conditions (V/III flux ratio = 1.0).

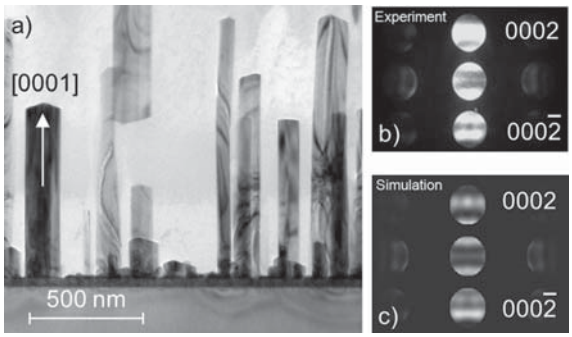

FIG. 5. (a) TEM image of GaN nanowires grown on a slightly N-rich AlN buffer layer (V/III flux ratio = 1.3). Also shown are experimental (b) and simulated (c) CBED diffraction patterns showing the Ga-polarity of a long nanowire. The CBED pattern was calculated for a sample thickness of 38 nm.

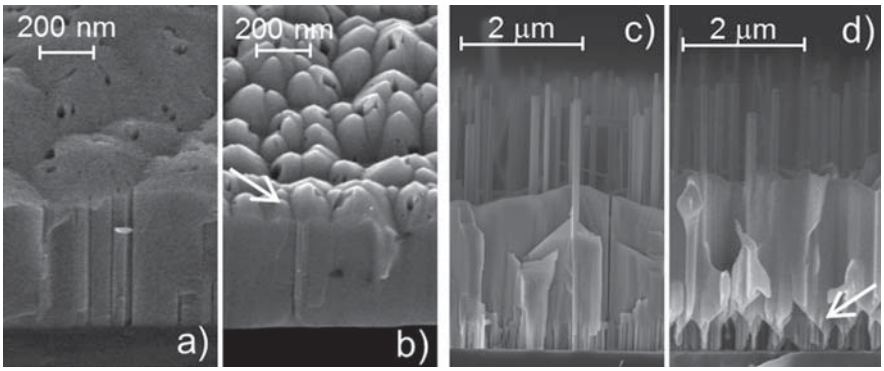

FIG. 6. FESEM images of low temperature GaN nanowire growth on N-polar [(a)-(b)] and Al-polar [(c)-(d)] AlN buffer layers showing the as-grown [(a) and (c)] and post-polarity-sensitive etched morphology [(b) and (d)]. The arrows indicate the N-face as determined from the emergence of pyramidal etch structures.

also a low density of nanowires observed (not shown). Polarity-sensitive etching reveals pyramidal structures on the top surface [Fig. 6(b)], indicating that the GaN matrix layer is in fact N-polar. We performed a similar low-temperature nanowire growth using a predominantly Al-polar AlN buffer film grown in another growth system. More aggressive etch conditions (125 °C, 60 s) were required for GaN, and etching would preferentially attack the AlN buffer layer, allowing the etchant to access the interface side of the GaN film. Consequently, pyramidal etch figures emerge at the interface surface underside of the GaN film, indicating Ga-polarity [Fig. 6(d)]. These experiments illustrate that the GaN matrix layer propagates the polarity of the underlying AlN film layer.

IV. CONCLUSIONS

The morphology of GaN nanowires was found to depend on the V/III flux ratio of the underlying low-temperature AlN buffer layer. AlN buffers grown under slightly N-rich conditions provided a favorable growth surface for straight, low-density, and coalescence-free nanowires that could be grown to arbitrary lengths. Diverging from this condition led to tilted nanowire growth for very N-rich AlN conditions or to large and highly irregular nanowires for Al-rich conditions, similar to the surface topography observed in associated AlN buffer layers. Polarity-sensitive etching and PFM measurements revealed that all AlN buffers in this study exhibited columnar protrusions with mixed polarity. Al-polar columns are speculated to act as nanowire nucleation sites, based on the similar size, shape, density, and polarity of GaN nanowires. The morphology and polarity of the resulting GaN nanowires suggests that Ga-polar growth rates are much higher than N-polar growth rates under typical nanowire growth conditions, leading to sparse nanowires for AlN buffer layers that are mostly N-polar with isolated Al-polar columns.

ACKNOWLEDGMENTS

Financial support for this research was provided by the National Institute of Standards and Technology (NIST). Partial support was provided by the DARPA Center on Nanoscale Science and Technology for Integrated Micro/Nano-Electromechanical Transducers (iMINT) and the DARPA N/MEMS S&T Fundamentals program under Grant No. N66001-10-1-4007, issued by the Space and Naval Warfare Systems Center Pacific (SPAWAR). The authors thank Sandra W. Claggett for TEM specimen preparation.

[1]E. Calleja, M. A. Sanchez-Garcia, F. J. Sanchez, F. Calle, F. B. Naranjo, E. Munoz, S. I. Molina, A. M. Sanchez, F. J. Pacheco, and R. Garcia, J. Cryst. Growth **201**, 296 (1999).
[2]G. Koblmueller, R. Averbeck, L. Geelhaar, H. Riechert, W. Hosler, and P. Pongratz, J. Appl. Phys. **93**, 9591 (2003).
[3]U. Kaiser, P. D. Brown, I. Khodos, C. J. Humphreys, H. P. D. Schenk, and W. Richter, J. Mater. Res. **14**, 2036 (1999).
[4]K. A. Bertness, A. Roshko, L. M. Mansfield, T. E. Harvey, and N. A. Sanford, J. Cryst. Growth **300**, 94 (2007).
[5]O. Landre, C. Bougerol, H. Renevier, and B. Daudin, Nanotechnology **20**, 8 (2009).
[6]J. Ristic, E. Calleja, S. Fernández-Garrido, L. Cerutti, A. Trampert, U. Jahn, and K. H. Ploog, J. Cryst. Growth **310**, 4035 (2008).
[7]H. Sekiguchi, T. Nakazato, A. Kikuchi, and K. Kishino, J. Cryst. Growth **300**, 259 (2007).
[8]V. Consonni, M. Knelangen, L. Geelhaar, A. Trampert, and H. Riechert, Phys. Rev. B **81**, 10 (2010).
[9]X. Q. Shen, T. Ide, S. H. Cho, M. Shimizu, S. Hara, H. Okumura, S. Sonoda, and S. Shimizu, J. Cryst. Growth **218**, 155 (2000).
[10]A. Yoshikawa and K. Xu, Opt. Mater. **23**, 7 (2003).
[11]F. Zhong, K. Qiu, X. H. Li, Z. J. Yin, X. J. Xie, Y. Wang, C. J. Ji, X. C. Cao, Q. F. Han, J. R. Chen, and Y. Q. Wang, Chin. Phys. Lett. **24**, 240 (2007).
[12]V. Lebedev, B. Schroter, G. Kipshidze, and W. Richter, J. Cryst. Growth **207**, 266 (1999).
[13]S. Dasgupta, F. Wu, J. S. Speck, and U. K. Mishra, Appl. Phys. Lett. **94**, 3 (2009).
[14]D. Cherns, L. Meshi, I. Griffiths, S. Khongphetsak, S. V. Novikov, N. Farley, R. P. Campion, and C. T. Foxon, Appl. Phys. Lett. **92**, 3 (2008).
[15]C. T. Foxon, S. V. Novikov, J. L. Hall, R. P. Campion, D. Cherns, I. Griffiths, and S. Khongphetsak, J. Cryst. Growth **311**, 3423 (2009).
[16]B. L. VanMil, H. C. Guo, L. J. Holbert, K. Lee, T. H. Myers, T. Liu, and D. Korakakis, J. Vac. Sci. Technol. B **22**, 2149 (2004).
[17]A. J. Ptak, T. H. Myers, L. T. Romano, C. G. Van de Walle, and J. E. Northrup, Appl. Phys. Lett. **78**, 285 (2001).
[18]B. J. Rodriguez, A. Gruverman, A. I. Kingon, and R. J. Nemanich, J. Cryst. Growth **246**, 252 (2002).
[19]R. Calarco, R. Meijers, T. Stoica, and H. Lüth, Phys. Status Solidi A **202**, 785 (2005).
[20]T. Stoica, R. Calarco, R. Meijers, and H. Lüth, Appl. Surf. Sci. **253**, 4300 (2007).
[21]K. A. Bertness, A. Roshko, L. M. Mansfield, T. E. Harvey, and N. A. Sanford, J. Cryst. Growth **310**, 3154 (2008).
[22]D. Zhuang and J. H. Edgar, Mater. Sci. Eng. R. **48**, 1 (2005).
[23]J. Jasinski, Z. Liliental-Weber, Q. S. Paduano, and D. W. Weyburne, Appl. Phys. Lett. **83**, 2811 (2003).
[24]S. V. Kalinin, in *Nanoscale Characterisation of Ferroelectric Materials: Scanning Probe Microscopy Approach*, edited by M. Alexe and A. Gruverman (Springer-Verlag, Berlin, 2004).
[25]T. Takahashi and T. Kawamukai, Ultramicroscopy **82**, 63 (2000).

[26]S. Hong, J. Woo, H. Shin, J. U. Jeon, Y. E. Pak, E. L. Colla, N. Setter, E. Kim, and K. No, J. Appl. Phys. **89**, 1377 (2001).
[27]R. Nath, S. Hong, J. A. Klug, A. Imre, M. J. Bedzyk, R. S. Katiyar, and O. Auciello, Appl. Phys. Lett. **96**, 3 (2010).
[28]H. P. D. Schenk, G. D. Kipshidze, U. Kaiser, A. Fissel, J. Krausslich, J. Schulze, and W. Richter, J. Cryst. Growth **200**, 45 (1999).
[29]R. K. Debnath, R. Meijers, T. Richter, T. Stoica, R. Calarco, and H. Luth, Appl. Phys. Lett. **90**, 3 (2007).